# Characterization and Kinetic Mechanism of Catalytic Domain of Human Vascular Endothelial Growth Factor Receptor-2 Tyrosine Kinase (VEGFR2 TK), a Key Enzyme in Angiogenesis

Camran V. Parast,* Barbara Mroczkowski, Chris Pinko, Shawn Misialek, Godrej Khambatta, and Krzysztof Appelt

*Agouron Pharmaceuticals, Incorporated, 4215 Sorrento Valley Boulevard, San Diego, California 92121*

*Received June 1, 1998; Revised Manuscript Received October 1, 1998*

ABSTRACT: Vascular endothelial growth factor (VEGF) is a dimeric protein which induces formation of new blood vessels (angiogenesis) through binding to VEGF-receptor-2 tyrosine kinase (VEGFR2 TK) or KDR (kinase insert domain-containing receptor) on the surface of endothelial cells. Angiogenesis has been shown to be essential for malignancy of tumors; therefore, VEGFR2 TK is a potential therapeutic target for the treatment of cancer. Sequence homology studies indicate that VEGFR2 TK contains three domains: extracellular (ligand-binding domain), transmembrane, and intracellular (catalytic domain). In this work, the catalytic domain of VEGFR2 TK was cloned and expressed in a soluble active form using a baculovirus expression system. In the absence of ligand, the enzyme is shown to catalyze its autophosphorylation in a time-dependent and enzyme-concentration-dependent manner, consistent with a trans mechanism for this reaction. Mass spectrometry analysis revealed incorporation of $5.5 \pm 0.5$ mol of phosphate/mole of enzyme (monomer). In addition, the enzyme was shown to catalyze phosphorylation of a synthetic peptide, poly($E_4Y$). Using poly($E_4Y$) as substrate, the kinetic constants of both native and phosphorylated enzyme were determined. Enzyme phosphorylation increased catalytic efficiency of the enzyme by at least an order of magnitude. Furthermore, the enzyme was shown to catalyze the reverse reaction using phospho-poly($E_4Y$) as substrate. $Cd^{2+}$ was found to be an inhibitor of the enzyme. Kinetic studies revealed that inhibition by $Cd^{2+}$ was competitive with respect to $Mg^{2+}$ and noncompetitive with respect to MgATP. These results indicate that $Cd^{2+}$ competes for a second metal-binding site. Therefore, the reaction catalyzed by this enzyme was treated as a terreactant system. The kinetic mechanism of VEGFR2 TK was elucidated through the use of steady-state kinetic studies. According to these studies, the enzyme binds $Mg^{2+}$ and MgATP in a random fashion followed by ordered addition of the peptide substrate. The release of product is also ordered, with MgADP being released last. The order of substrate binding was confirmed by using AMP−PCP, a dead-end inhibitor.

Angiogenesis, a process by which new blood vessels form from pre-existing ones, is one of the essential processes in reproduction, development, and wound repair (*1*, *3*, *5*). Unregulated angiogenesis is associated with many diseases, such as; arthritis, diabetes, ocular vascularization, tumor growth, and metastasis (*2*, *3*, *5*). Therefore, inhibition of angiogenesis is considered a major target for development of therapeutic drugs.

Vascular endothelial growth factor (VEGF)[1] is one of the key players in angiogenesis. VEGF is a homodimeric glycoprotein (34−46 kDa) whose amino acid sequence is 20% identical to that of platelet-derived growth factor, including eight conserved cysteine residues (*16*). VEGF is thought to exert its angiogenic effect via binding to its receptor (VEGF-receptor-2 tyrosine kinase, VEGFR2 TK) on the surface of endothelial cells. VEGFR2 TK, or *kinase* insert *domain*-containing *receptor* (KDR), has been shown to play a key role in angiogenesis (*4*).

According to sequence homology studies, VEGFR2 TK is composed of an extracellular ligand-binding region, a single short membrane-spanning sequence, and an intracellular region containing a putative tyrosine kinase domain (*16*). On the basis of studies with similar receptors of this type, VEGFR2 TK is hypothesized to undergo dimerization upon binding to VEGF, resulting in its activation. Upon activation, the receptor is thought to initiate a cascade of phosphorylation which eventually leads to vascularization (*8*). Therefore, VEGFR2 TK is recognized as the target for the development of therapeutic drugs against angiogenesis.

A considerable amount of difficulty is often associated with studies of whole receptors due to the complexity of their structure, the interactions between different domains within the receptor molecule, and association with the membrane. However, recent studies on insulin receptor tyrosine kinase (IRTK) and other related receptors have suggested that the catalytic core of these receptors can be expressed separately as a soluble active enzyme (*6*−*9*). Expression of the catalytic domain greatly simplifies the study of these receptors since complex interactions between different regions are eliminated. Therefore the catalytic core fragment can be studied separately. Assuming that the catalytic properties of the soluble enzyme reflect those of

* To whom correspondence should be addressed. E-mail: parast@agouron.com. Tel: (619)-622-7920. Fax: (619)-678-8277.

10.1021/bi981291f CCC: $15.00 
Published on Web 11/05/1998

the intact receptor, information obtained from studies with the soluble fragment may be extended to the whole receptor.

We have cloned and expressed a fragment containing the catalytic core of human VEGFR2 TK (cchVEGFR2 TK) as a soluble active enzyme. Here in this work we report the characterization of the tyrosine kinase activity of this enzyme as well as the elucidation of its kinetic mechanism.

## MATERIALS AND METHODS

*Materials.* All of the chemicals were obtained from Sigma or Aldrich and were used without further purification. [$\gamma$-$^{33}$P]ATP was purchased from DuPont NEN. The peptide RDIYKDPDYVRK was purchased from American Peptide Company. All chromatography columns were purchased from Pharmacia Biotech.

*Enzymatic Synthesis of Phospho-poly($E_4Y$).* Phospho-poly($E_4Y$) was generated enzymatically by incubation of poly($E_4Y$) with cchVEGFR2 TK. The enzyme (150 nM, or 0.06 units/mL) was incubated with poly($E_4Y$) (5 mM), $MgCl_2$ (20 mM), ATP (1 mM), and DTT (5 mM) in a final reaction volume of 200 mL in Hepes (200 mM, pH 7.5). The reaction mixture was placed in dialysis tubing (1 kDa cutoff) and then in 4 L of solution containing $MgCl_2$ (20 mM), ATP (1 mM), and DTT (5 mM) to allow the reaction to go to completion by removing ADP generated and replenishing ATP. The reaction was carried out at room temperature for 5 h. The reaction was stopped by addition of an equal volume of 10% trichloroacetic acid (TCA) to precipitate poly($E_4Y$) and phospho-poly($E_4Y$). The precipitate was pelleted by centrifugation at 10 000 rpm (16490*g*) for 10 min at room temperature and then lyophilized. Nearly quantitative recovery was achieved. The lyophilized solid was dissolved in Hepes (200 mM, pH 7.5) at a final concentration of 80 mM and stored at −20 °C. Enzymatic assay of the product in the forward reaction indicated that it contained ∼34% poly($E_4Y$), suggesting that the phosphorylation reaction went 66% to completion. The presence of phospho-poly($E_4Y$) in the final product was indicated by the fact that it served as a substrate for the reverse reaction. As expected, poly($E_4Y$) was not a substrate for the reverse reaction. Thus, the final product was a mixture of poly($E_4Y$), 34%, and phospho-poly($E_4Y$), 66%. The product was used without further purification. The fraction of phosphotyrosine and tyrosine in the phospho-poly($E_4Y$) preparation was independently verified through spectral analysis and quantitation (276 and 266 nm for tyrosine and phosphotyrosine, respectively). These results indicated the presence of 30% nonphosphorylated tyrosine residues and 70% phosphorylated tyrosine residues in the phospho-poly($E_4Y$) preparations.

One unit is defined as the amount of enzyme which catalyzes the formation of one micromole of phospho-poly($E_4Y$) from poly($E_4Y$) in the presence of MgATP. The specific activity of the enzyme was 10 $\mu$mol min$^{-1}$ mg$^{-1}$.

*Construction of Baculovirus Transfer Vector*. The cDNA corresponding to the catalytic core VEGFR2 TK (amino acids 840−1192) was inserted into the baculovirus transfer vector pAcSG2. The upstream sequence flanking the translation initiation codon was engineered to contain the Kozak consensus sequence for the initiation of translation which has been demonstrated to enhance the expression of certain genes in the insect cell/baculovirus expression system. The nucleotide sequence of the baculovirus transfer vector was verified by dideoxy sequencing.

*Cell Culture*. Sf9 insect cells were cotransfected with the recombinant baculovirus transfer vector and linear baculovirus DNA (BaculoGold AcMNPV DNA, Pharmingen, San Diego, CA). Recombinant virus particles containing the cchVEGFR2 TK sequence inserted under the regulation of the strong polyhedrin promoter were plaque purified and amplified to a high titer in Sf9 cells.

*Purification of cchVEGFR2 TK.* Cell pellet (75 g) was suspended in Tris (20 mM), pH 8.0, DTT (5 mM), and NaCl (20 mM) and then sonicated. Lysate was centrifuged for 45 min at 35000*g*. The soluble fraction was loaded onto a Q-Sepherose fast-flow column (200 mL), and the protein was eluted with a NaCl gradient (20−600 mM) in Tris (20 mM, pH 8) and DTT (5 mM). Fractions containing the enzyme were pooled by SDS−PAGE analysis. The pooled sample was applied directly on to a Macroprep Hydroxyapatite column (110 mL). The enzyme was eluted by a potassium phosphate gradient (5−150 mM), pH 8, NaCl (150 mM), and DTT (5 mM). Fractions containing the enzyme were pooled and buffer exchanged into Tris (20 mM, pH 7.5), NaCl (20 mM), and DTT (5 mM). The enzyme sample was then loaded on to a mono-Q column (8 mL), and the enzyme was eluted with a NaCl gradient (20−200 mM) over 20 column volumes. The fractions containing the enzyme were pooled and concentrated using a 20 micron bead Macroprep Hydroxyapatite column (2 mL). The enzyme was eluted using a potassium phosphate gradient (5−125 mM), pH 7.5, NaCl (150 mM), and DTT (5 mM). The final pool was loaded onto a Superose 12 sizing column, and the enzyme was eluted with potassium phosphate buffer (100 mM), pH 7.5, and DTT (5 mM).

*Sequence Analysis of Tryptic Peptides.* Purified cch-VEGFR2 TK (100 pmol) was applied to a Prospin cartridge (Applied Biosystems Division of Perkin-Elmer). The poly(vinylidene difluoride) disk was removed from the ProSpin cartridge and washed in 20% ethanol prior to digestion with trypsin or endolys-C. Two HPLC fractions were analyzed by MALDI TOF mass spectrometry (Protein/Peptide Micro

[1] Abbreviations: VEGF, vascular endothelial growth factor; DTT, dithiothreitol; Tris, Tris-(hydroxymethyl) amino-methane; Hepes, (*N*-[2-hydroxyethyl]piperazine-*N*′-[2-ethanesulfonic acid]); PDGF, platelet-derived growth factor; VEGFR2 TK, vascular endothelial growth factor receptor-2 tyrosine kinase; cdVEGFR2 TK, cytosolic domain vascular endothelial growth factor receptor-2 tyrosine kinase; ccVEGFR2 TK, catalytic core vascular endothelial growth factor receptor-2 tyrosine kinase; p-cchVEGFR2 TK, phosphorylated catalytic core of human vascular endothelial growth factor receptor-2 tyrosine kinase; cch-VEGFR2 TK, catalytic core of human vascular endothelial growth factor receptor-2 tyrosine kinase; IRTK, insulin receptor tyrosine kinase; cdIRTK, cytosolic domain insulin receptor tyrosine kinase; ccIRTK, catalytic core insulin receptor tyrosine kinase; aFGF, acidic fibroblast growth factor; bFGF, basic fibroblast growth factor; TNF, tumor necrosis factor; KDR, kinase *insert* domain-*containing* receptor; Flt-1, *f* ms-like tyrosine *kinase*; poly($E_4Y_1$), poly(Glu, Tyr) 4:1; TCA, trichloroacetic acid; ATP, adenosine 5′-triphosphate; CPM, counts per minute; DPM, disintegration per minute; SDS−PAGE, sodium dodecyl sulfate−polyacrylamide gel electrophoresis; PEP, phosphoenol pyruvate; LDH, lactic dehydrogenase; PK, pyruvate kinase; HK, hexokinase; NAD, $\beta$-nicotinamide adenine dinucleotide; NADH, $\beta$-nicotinamide adenine dinucleotide, reduced form; cAPK, cAMP-dependent protein kinase; cAMP, cyclic adenosine 5′-monophosphate; AMP−PNP, 5′-adenylylimidodiphosphate ($\beta$, $\gamma$-imidoadenosine 5′-triphosphate); AMP−PCP, $\beta$, $\gamma$-methyleneadenosine 5′-triphosphate (adenylmethylenediphosphonate).

Analytical Laboratory, California Institute of Technology). Both peptides aligned with the human VEGF-R2 sequence deposited in the nucleic acid data banks.

*Radioactive Tyrosine Kinase Assays.* The assays were performed in Hepes (200 mM), pH 7.5, DTT (5 mM), $MgCl_2$ (25 mM), poly($E_4Y_1$) (500−600 $\mu$g/mL, 0.8−1 mM Tyr), [$\gamma$-$^{33}$P]ATP (1000−3000 Ci/mmol), 0.2−2 $\mu$Ci per reaction, 2−400 $\mu$M unlabeled ATP, and 40 nM cchVEGFR2 TK in final volume of 50 $\mu$L in 1.5 mL Eppendorf tubes at room temperature. The formation of product was monitored by quantitating the incorporation of radiolabel into the substrate by two different methods: precipitation by 10% TCA for poly($E_4Y$) and filter paper binding for small peptides.

*Product Detection by Precipitation.* The reactions were typically quenched after 10−15 min by addition of 80 $\mu$L of 10% TCA. The precipitate, poly($E_4Y$) and the enzyme, was pelleted by centrifugation at 14000 rpm (16000*g*) for 4 min, the supernatant was discarded, the pellet was washed with 90 $\mu$L of 10% TCA and centrifuged at 14000 rpm (16000*g*) for 4 min, supernatant was discarded, and the pellet was dissolved in Tris (1 M, pH 7.5). The solution was transferred to liquid scintillation (5 mL) for liquid scintillation counting (cpm), using a Wallace 1409 Liquid Scintillation Counter. A quench library was generated for $^{33}$P, for dpm measurements, but quenching was found to be minimal under the experimental conditions. Each vial was counted for 60 s. The enzyme activity was essentially linear under the experimental conditions.

*Product Detection by Filter Paper Binding.* The reactions were quenched by the addition of 50 $\mu$L of 8% phosphoric acid. The reaction mixture was vortexed and applied onto a square P80 paper (2 cm × 2 cm). The papers were washed three times with 0.5% phosphoric acid and once with acetone. The papers were then transferred to scintillation vials, and the amount of radioactivity in each sample was quantitated by liquid scintillation counting as described above.

*Western Blot Analysis.* Western blot analysis was performed using a Novex western transfer apparatus. The experiment was performed according to the instructions provided by the manufacturer (Novex). Phosphorylated protein was detected through use of anti-phosphotyrosine (PY20) (1/1000 dilution) as the primary antibody and goat anti-mouse IgG horseradish peroxidase (1/2000 dilution) as the secondary antibody (Transduction Laboratories). The final visualization was performed using ECL Western Blotting Protocols (Amersham Life Science).

*Coupled Spectrophotometric Assay for the Forward Direction.* Tyrosine kinase assays were monitored using a Beckman DU 650 spectrophotometer. Production of ADP was coupled to oxidation of NADH using phosphoenolpyruvate (PEP) through the actions of pyruvate kinase (PK) and lactic dehydrogenase (LDH). The oxidation of NADH was monitored by following the decrease in absorbance at 340 nm ($\epsilon_{340}$ = 6.22 cm$^{-1}$ mM$^{-1}$). Typical reaction solutions contained the following: 1 mM PEP, 250 $\mu$M NADH, 20 units of LDH/mL, 40 units of PK/mL, and 5 mM DTT in 200 mM Hepes, pH 7.5, and varying concentrations of poly($E_4Y_1$), ATP, and $MgCl_2$. Assays were initiated with 40 nM cchVEGF−R2.

*Coupled Spectrophotometric Assay for the Reverse Reaction.* ATP generation was coupled to production of NADH via the action of hexokinase (HK) and glucose-6-phosphate dehydrogenase (G6PD). In this assay, HK catalyzes the conversion of ATP to ADP and glucose-6-phosphate. Glucose-6-phosphate is then oxidized to D-6-phosphogluconopyranose-1,5-lactone by G6PD with concomitant reduction of NAD to NADH which can be monitored at 340 nm. A typical assay solution contained the following: glucose (10 mM), NAD (40 mM), DTT (5 mM), $MgCl_2$ (4 mM), HK (15 units/mL), G6PD (15 units/mL), and indicated concentrations of ADP and phospho-poly($E_4Y$). The reactions were initiated with the addition of enzyme (600−900 nM).

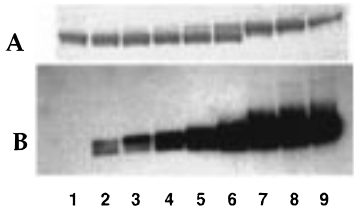


FIGURE 1: Time dependence of autophosphorylation. (A) SDS−PAGE of the enzyme samples incubated with MgATP for varying times: (1) 0, (2) 10 s, (3) 30 s, (4) 1 min, (5) 2 min, (6) 5 min, (7) 17 min, (8) 30 min, and (9) 45 min. (B) Western blot analysis of the samples in A.

*Data Analysis.* Initial rates were determined by a linear least-squares regression analysis of the change in absorbance as a function of time. The initial velocities as a function of substrate concentrations were fitted to equilibrium ordered, sequential, and ping-pong mechanisms using the equations from Cleland (*10*). Inhibition data were fitted to the equations for competitive, noncompetitive, and uncompetitive inhibition using Cleland equations (*10*).

## RESULTS

*Detection and Time Course of Autophosphorylation Reaction.* Autophosphorylation was monitored by western blot analysis using anti-phosphotyrosine antibody and horseradish peroxidase as outlined in Materials and Methods. It has been shown that phosphorylation of proteins is associated with a shift in their mobility on SDS−PAGE; the fully phosphorylated protein usually migrates at a slightly higher molecular weight than the nonphosphorylated form. Therefore, a SDS−PAGE shift in mobility can also be used to monitor the phosphorylation reaction.

To investigate the time course of the autophosphorylation reaction, the enzyme (10 $\mu$M) was incubated with MgATP (5 mM) at room temperature, and the reaction was quenched by addition of SDS at indicated time intervals. SDS−PAGE analysis of the samples demonstrated that, upon incubation of the enzyme with MgATP, there was a change in the mobility of the enzyme (Figure 1A). A SDS−PAGE shift in mobility of the protein upon incubation with MgATP was correlated with an increase in the phosphorylation state of the enzyme as judged by western blot analysis (Figure 1B). Taken together, these results indicate that the enzyme is capable of catalyzing its autophosphorylation. The starting enzyme was not phosphorylated. Under these conditions, autophosphorylation occurred in a time-dependent manner, being complete in 20 min. On the basis of altered SDS−PAGE mobility of the enzyme upon phosphorylation, multiple phosphorylated species could be detected.

*Effect of MgATP Concentration on Autophosphorylation Reaction.* To determine the optimal ATP concentration in

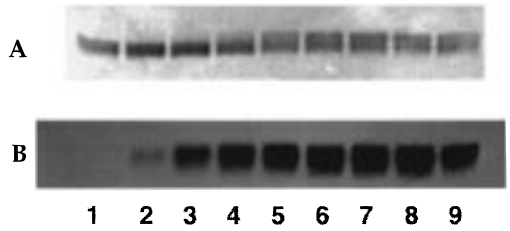


FIGURE 2: The effect of MgATP concentrations on the rate of autophosphorylation reaction. (A) SDS−PAGE of the enzyme samples (10 $\mu$M) incubated with varying concentrations of MgATP for 5 min at room temperature. The concentrations of MgATP were (1) 0, (2) 100 $\mu$M, (3) 200 $\mu$M, (4) 500 $\mu$M, (5) 1 mM, (6) 2 mM, (7) 5 mM, (8) 10 mM, and (9) 20 mM. (B) Western blot analysis of the samples in A.

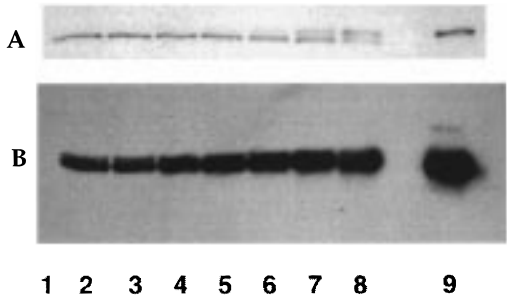


FIGURE 3: The effect of enzyme concentration on the rate of autophosphorylation reaction. (A) SDS−PAGE of varying concentrations of enzyme incubated with 5 mM MgATP at 4 °C. The concentrations of the enzyme were (1) 0, (2) 1.8 $\mu$M, (3) 2.5 $\mu$M, (4) 3.6 $\mu$M, (5) 5 $\mu$M, (6) 7 $\mu$M, (7) 10 $\mu$M, (8) 14 $\mu$M, and (9) 20 $\mu$M. An equal amount of protein was loaded into each well. (B) Western blot of samples in A. Lane 1 contained enzyme incubated with 0 ATP as a control for the nonphosphorylated starting enzyme sample.

autophosphorylation reaction, the same concentration of the enzyme (10 $\mu$M) was incubated with varying concentrations of ATP at room temperature for 5 min. The reactions were quenched by the addition of SDS followed by quantitation via western blot as stated in the Materials and Methods section. There is a direct relationship between the rate of autophosphorylation and the concentration of MgATP (Figure 2). No attempt was made to determine $K_{M(MgATP)}$ in this reaction (see below).

*Mechanism of Autophosphorylation.* There are at least two possible mechanisms for autophosphorylation: trans and cis. In a trans mechanism, one receptor molecule serves as the substrate while the other molecule serves as the enzyme. In a cis mechanism, the same molecule catalyzes its own phosphorylation; that is, part of the molecule serves as the substrate for the active site of the same molecule. Although there are no direct ways of distinguishing between these two mechanisms, a trans mechanism of autophosphorylation predicts that autophosphorylation should be enzyme-concentration-dependent while a cis mechanism is expected to be enzyme-concentration-independent.

To address the mechanism of autophosphorylation, we incubated different concentrations of enzyme with MgATP under identical conditions at 4 °C for 5 min. The reactions were quenched by the addition of SDS, and phosphorylation was quantified by Western Blot analysis (Figure 3). The rate of autophosphorylation was dependent on enzyme concentration. Inhibition was observed at enzyme concentrations above 20 $\mu$M. Our results clearly demonstrate that cchVEGFR2 TK is capable of undergoing autophosphorylation in the presence of MgATP in an enzyme-concentration-dependent manner. Direct correlation between autophosphorylation and enzyme concentration suggests a trans mechanism for this reaction.

*Number of Phosphorylation Sites.* Neither western blot analysis nor SDS−PAGE addresses the number of phosphoryl groups per molecule of enzyme quantitatively. To establish the number of phosphorylation sites per molecule, the enzyme (20 $\mu$M) was incubated with MgATP to yield fully phosphorylated enzyme. Mass spectrometry analysis of the sample indicated that the phosphorylated form exhibited a higher mass relative to that of the nonphosphorylated form (data not shown). The increase in mass of the phosphorylated form relative to the nonphosphorylated form corresponded to 5.5 ± 0.5 phosphate groups/molecule of enzyme, indicating that there are 5−6 phosphorylation sites/molecule of the enzyme.

Previous work with bacterially expressed full-length cytosolic domains of human VEGFR2 TK has identified at least four phosphorylation sites (*11*). Our results are consistent with those findings and further indicate the presence of additional site(s) which were not detected in the bacterially expressed enzyme. This discrepancy may be due to misfolding of the bacterially expressed enzyme since it was found to be highly aggregated.

*Tyrosine Kinase Activity Versus Exogenous Substrate.* In addition to catalyzing its autophosphorylation, cchVEGFR2 TK was also capable of catalyzing phosphate transfer from ATP to an exogenous substrate (eq 1). Since the physiological substrate for this enzyme has not yet been identified, two synthetic peptides were used as substrates: a peptide (RDIYKDPDYVRK) derived from one of the autophosphorylation sites (activation loop) on the enzyme, and a synthetic peptide, poly($E_4Y$), which is a random copolymer of glutamic acid and tyrosine. Since poly($E_4Y$) was more efficiently phosphorylated by VEGFR2 TK than the activation loop peptide, poly($E_4Y$) was used as the exogenous substrate in all subsequent studies. The phosphorylation reaction was monitored by two different methods (eq 1). By using a direct, discontinuous radioactive assay, we monitored the transfer of radiolabel from [$\gamma$-$^{33}$P]ATP to the peptide substrate. By using a continuous coupled spectrophotometric assay, we monitored the generation of ADP. Enzyme-specific activities measured using both assays were identical, indicating that ATP hydrolysis was tightly coupled to the generation of phosphopeptide. No futile ATPase activity was detected.

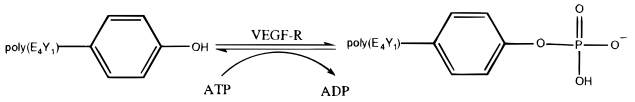


(1)

*Determination of the Optimal Conditions for Tyrosine Kinase Activity.* By using poly($E_4Y$) as the substrate, we tested the effects of different conditions on the enzymatic activity of the enzyme. The profile of enzyme activity versus pH indicated that the enzyme was active between pH 7 and 8, with the optimal activity at pH 7.5. The enzyme activity declined sharply below and above pH 7 and 8, respectively (data not shown). The effects of two salts on the enzyme

Table 1

| | native cchVEGF-R2 | | | phosphorylated cchVEGF-R2 | | |
|---|---|---|---|---|---|---|
| substrate | $K_M$ (mM) | $k_{cat}$ ($s^{-1}$) | $k_{cat}/K_M$ ($s^{-1}$ $M^{-1}$) | $K_M$ (mM) | $k_{cat}$ ($s^{-1}$) | $k_{cat}/K_M$ ($s^{-1}$ $M^{-1}$) |
| Forward Reaction | | | | | | |
| MgATP | 0.6 | 5 | $8.3 \times 10^3$ | 0.150 | 12 | $80 \times 10^3$ |
| poly($E_4$Y) | 9.4 | | $5.3 \times 10^2$ | 2 | | $60 \times 10^2$ |
| $Mg^{2+}$ | 30 | | $1.7 \times 10^2$ | 6.7 | | $17 \times 10^2$ |
| Reverse Reaction | | | | | | |
| MgADP | 0.15 | 0.1 | $6.7 \times 10^2$ | 0.05 | 0.13 | $26 \times 10^2$ |
| P-poly($E_4$Y) | 3 | | $3.3 \times 10^1$ | 0.7 | | $18 \times 10^1$ |

activity was tested. Both NaCl and $(NH_4)_2SO_4$ were found to inhibit the activity in a concentration-dependent manner, leading to complete inhibition at concentrations above 500 and 250 mM for NaCl and $(NH_4)_2SO_4$, respectively (data not shown). Both native and phosphorylated forms of the enzyme exhibited similar properties in all of the experiments mentioned above.

In reactions in which phosphorylated cchVEGFR2 TK (p-cchVEGFR2 TK) was used, the nonphosphorylated enzyme was phosphorylated by incubation with MgATP under conditions which resulted in full phosphorylation of the enzyme (10−20 $\mu$M enzyme, see above). Excess $Mg^{2+}$ and ATP were removed by dialysis to obtain pure phosphorylated cchVEGFR2 TK. The p-cchVEGFR2 TK was found to be more stable than cchVEGFR2 TK under our experimental conditions (data not shown). The phosphorylated enzyme was frozen at −70 °C, and aliquots were taken out for enzyme activity assays. No dephosphorylation was detected under our experimental conditions (data not shown).

*Forward Reaction.* Kinetic constants for the forward reaction are summarized in Table 1. All kinetic constants were determined using the spectrophotometric assay (see Materials and Methods). Phosphorylation of the enzyme significantly alters the kinetic constants of the enzyme: the phosphorylated form of the enzyme exhibits higher $k_{cat}$ and lower $K_M$ values for all of its substrates. Phosphorylation of the enzyme increases its catalytic efficiency ($k_{cat}/K_M$) by a factor of 10 for all substrates, compared to the native form.

*Reverse Reaction.* Production of ATP was monitored. All kinetic constants were determined using the spectrophotometric assay for the reverse reaction (see Materials and Methods). Incubation of the enzyme with phospho-poly-($E_4$Y), ADP, and $Mg^{2+}$ resulted in the generation of ATP, indicating that the enzyme is capable of catalyzing the reverse reaction. The kinetic constants for the reverse reaction are summarized in Table 1. As in the forward direction, enzyme phosphorylation results in a decrease in its $K_M$ for both substrates and a slight increase in its $k_{cat}$.

It should be noted that the presence of ∼35% nonphosphorylated poly($E_4$Y) in the phospho-poly($E_4$Y) preparation could confound evaluation of the reverse reaction kinetics. Since nonphosphorylated poly($E_4$Y) is presumably an inhibitor of the reverse reaction, it might effectively compete with phospho-poly($E_4$Y) for binding to the enzyme, although a comparison of the affinity of poly($E_4$Y), $K_{M(poly(E4Y))} = 9.4$ mM, and phospho-poly($E_4$Y), $K_{M(p-poly(E4Y))} = 3$ mM, would suggest that this effect might not be significant.

*Metal Requirements.* The kinase activity was found to have an absolute requirement for metals. Both $Mg^{2+}$ and $Mn^{2+}$ were found to be able to support enzyme activity. Optimal activity was observed at 25 and 2 mM for $Mg^{2+}$ and $Mn^{2+}$, respectively. $V_{max}$ was 2-fold higher in the presence of $Mg^{2+}$ relative to that in the presence of $Mn^{2+}$ at optimal concentrations of each metal. Both metals inhibited the enzymatic activity at concentrations over 25 and 2 mM for $Mg^{2+}$ and $Mn^{2+}$, respectively (data not shown).

It is generally believed that, in all ATP utilizing enzymes, MgATP, rather than ATP alone, serves as the actual substrate (*12*). The function of $Mg^{2+}$ is to chelate to ATP forming MgATP, the cognate substrate. However, it has been shown that some enzymes require $Mg^{2+}$ concentrations in excess of that which is necessary for chelation to ATP to form MgATP (*13*, *14*). These results have generally been taken as evidence for the existence of a second metal-binding site on the enzyme. However, no direct evidence has been found in support of the second metal-binding site since these enzymes can be purified in a metal-free form. Thus, in these cases, $Mg^{2+}$ plays two roles: chelation to ATP to form MgATP and binding to another site whose function is generally to assist in catalysis.

In the case of cchVEGFR2 TK, the concentration of $Mg^{2+}$ required for enzyme activity (25 mM) far exceeds that which is required for chelation to ATP to form MgATP (*15*). Therefore, it appears likely that $Mg^{2+}$ plays a dual role in this reaction: in addition to chelation to ATP, it binds to a second site whose binding is necessary for catalysis. To verify the existence of a second binding site for $Mg^{2+}$, a series of divalent metals were tested for their inhibitory properties against $Mg^{2+}$. $Cd^{2+}$, $Co^{2+}$, and $Ca^{2+}$ were found to inhibit the enzyme activity.

*Kinetics of Enzyme Inhibition by $Cd^{2+}$.* There are several possible mechanisms for enzyme inhibition by $Cd^{2+}$. $Cd^{2+}$ might chelate to ATP to form CdATP which could compete with MgATP for the enzyme active site, leading to inhibition of enzyme activity, assuming that CdATP is not a substrate or that it is a slow substrate for the enzyme. Another possibility is that $Cd^{2+}$ may compete with $Mg^{2+}$ for the putative second metal-binding site on the enzyme. Kinetic studies may be used to distinguish between these two possible mechanisms. If $Cd^{2+}$ competes with $Mg^{2+}$ for a second metal-binding site, $Cd^{2+}$ would be expected to be a competitive inhibitor with respect to $Mg^{2+}$ and a noncompetitive inhibitor with respect to MgATP.

These experiments may be rather difficult to interpret because MgATP and CdATP would be expected to interconvert readily if the concentrations of $Cd^{2+}$ and $Mg^{2+}$ are similar. However, since $Cd^{2+}$ is a relatively potent inhibitor of the enzyme ($K_I = 15$ $\mu$M), these experiments can be carried out in the presence of ∼1000-fold excess $Mg^{2+}$ relative to $Cd^{2+}$ such that the concentration of $Mg^{2+}$ remains essentially constant throughout the experiment.

Thus, to address the mechanism of inhibition by $Cd^{2+}$, inhibition studies were conducted in the presence of several fixed concentrations of $Cd^{2+}$ (0, 10, and 20 $\mu$M) with $Mg^{2+}$ as the varying substrate (4−25 mM) at a fixed concentration of ATP (1 mM). The $Mg^{2+}$ concentrations used in these studies are quite reasonable since the enzyme exhibits little activity at $Mg^{2+}$ concentrations below 4 mM. Under these conditions, there is a 200−1250-fold excess of $Mg^{2+}$ over $Cd^{2+}$. $Cd^{2+}$ exhibits an affinity to ATP that is ∼5-fold higher than that of $Mg^{2+}$ (data not shown). Therefore, under our conditions, $Cd^{2+}$ would not be able to effectively compete

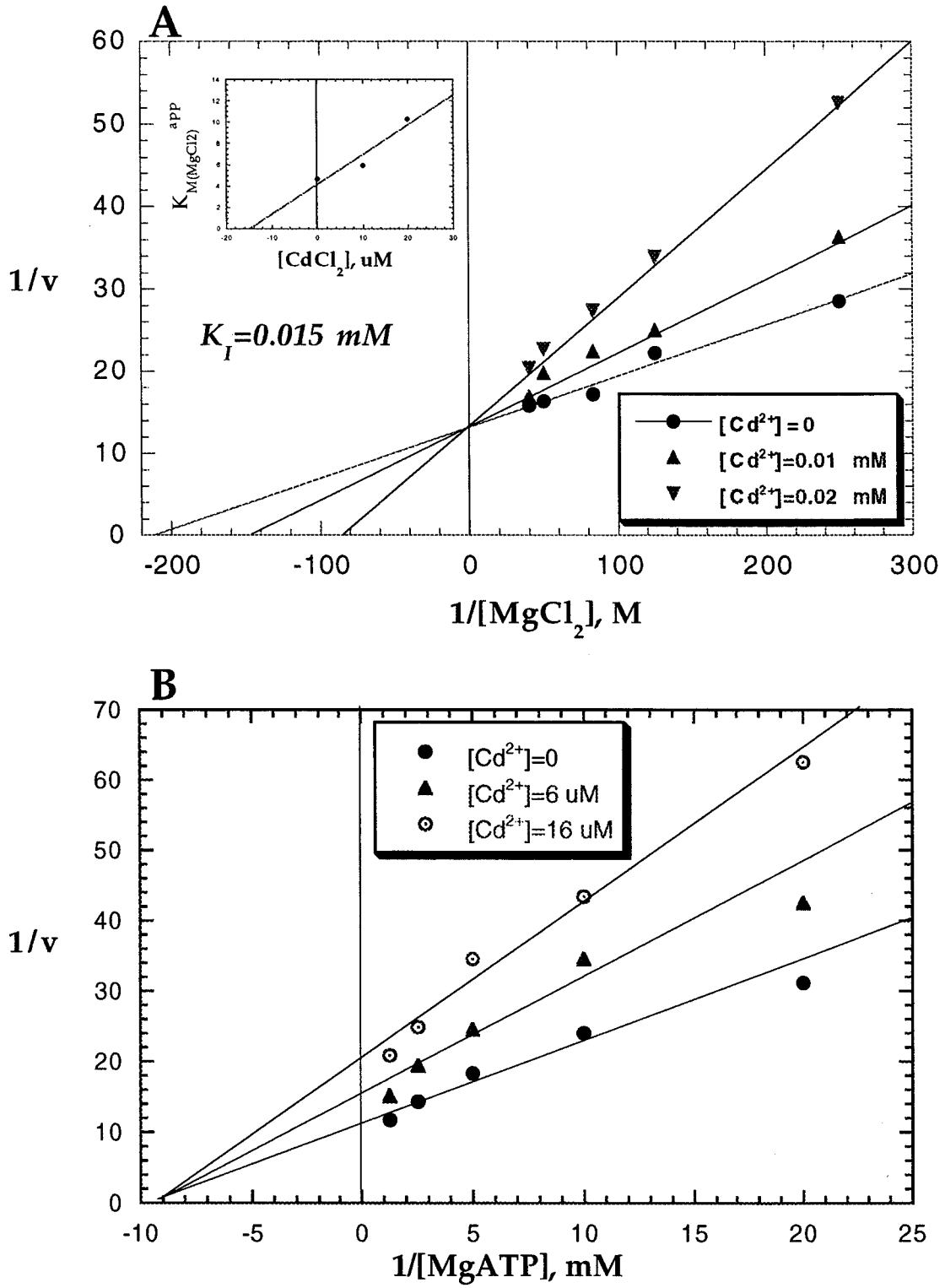


FIGURE 4: Kinetics of enzyme inhibition by $Cd^{2+}$. (A) Plot of $1/v$ vs $1/[Mg^{2+}]$ at three fixed concentrations of $Cd^{2+}$ and one fixed concentration of MgATP, 1 mM, and poly($E_4Y_1$), 500 $\mu$g/mL. (B) Plot of $1/v$ vs 1/[MgATP] at three fixed concentrations of $Cd^{2+}$ and one fixed concentration of $Mg^{2+}$, 25 mM, and poly($E_4Y_1$), 500 $\mu$g/mL. The unit for velocity ($v$) is expressed in $\Delta OD_{@340\ nm}$/min.

with $Mg^{2+}$ for the formation of CdATP. In addition, the maximum concentration of CdATP can be no greater than 20 $\mu$M. Given these conditions, it is reasonable to assume that the concentration of $Mg^{2+}$ will not be affected significantly during the experiment and would remain relatively constant, which makes the interpretations of the experiment relatively straightforward. The pattern of inhibition clearly indicates that $Cd^{2+}$ is a competitive inhibitor with respect to $Mg^{2+}$ (Figure 4A), indicating that $Cd^{2+}$ competes with $Mg^{2+}$ for the same site on the enzyme.

In a second experiment, inhibition studies were performed in the presence of several fixed concentrations of $Cd^{2+}$ (0, 6, and 16 $\mu$M) with ATP as the varying substrate (50−800 $\mu$M) at a fixed concentration of $Mg^{2+}$ (20 mM). Under these conditions, there is a 1250−3000-fold excess of $Mg^{2+}$ over $Cd^{2+}$. Again, $Cd^{2+}$ would not be able to effectively compete

with $Mg^{2+}$ for formation of CdATP. Therefore, the concentration of $Mg^{2+}$ would remain relatively constant throughout the experiment. By the same reasoning, most of the ATP would exist as MgATP under these conditions, due to a large excess of $Mg^{2+}$ over $Cd^{2+}$. Under these conditions, MgATP can be identified as the varying species. Thus, when MgATP is the varying substrate, the pattern of enzyme inhibition by $Cd^{2+}$ is noncompetitive (Figure 4B), indicating that $Cd^{2+}$ does not compete with MgATP for the same binding site. These results, taken together, indicate that $Cd^{2+}$ inhibits the enzyme activity by competing with $Mg^{2+}$ for a second metal-binding site.

Although the second metal functions not as a substrate but as an essential activator of the enzyme, the reaction catalyzed by cchVEGFR2 TK was treated as a terreactant system for the determination of the kinetic mechanism of the enzyme.

*Substrate Kinetics.* Initial velocity studies were undertaken on the reaction catalyzed by cchVEGFR2 TK using MgATP, $Mg^{2+}$, and poly($E_4Y$). The coupled spectrophotometric assay was used in all of these studies. The phosphorylated form of the enzyme was used in all of these experiments due to its higher activity. Phosphorylated enzyme was prepared as described above.

Six families of lines were generated by keeping the concentration of one of the substrates constant while varying the concentration of the second substrate at several fixed concentrations of the third substrate. Double reciprocal plots are presented (Figures 5, 6, and 7). Initial velocity line patterns were all intersecting, indicating a sequential mechanism. These results clearly rule out a ping-pong mechanism where a parallel line pattern would be expected.

When $1/v$ is plotted versus 1/poly($E_4Y$) at several fixed concentrations of MgATP, keeping $Mg^{2+}$ concentration constant (Figure 5A), the pattern crosses on the vertical axis. When $1/v$ is plotted versus 1/MgATP at several fixed concentrations of poly($E_4Y$), keeping $Mg^{2+}$ concentration constant (Figure 5B), the pattern intersects to the left of the vertical axis and above the horizontal one. A replot of slopes versus 1/poly($E_4Y$) (Figure 5B, inset) goes through the origin, indicating that $K_{M(MgATP)}$ has become 0 (or very small compared to $K_{i(MgATP)}$). These results clearly indicate that binding of the two substrates, MgATP and poly($E_4Y$), is ordered with MgATP binding first. In other words, poly($E_4Y$) cannot add except to E*MgATP; and conversely, MgATP cannot dissociate from E*MgATP* poly($E_4Y$), but only from E*MgATP. These results are clearly inconsistent with a random addition of substrates in which case an identical pattern would be predicted when $1/v$ is plotted versus 1/poly($E_4Y$) or when $1/v$ is plotted versus 1/MgATP.

When $1/v$ is plotted versus $1/Mg^{2+}$ at several fixed concentrations of MgATP, keeping poly($E_4Y$) concentration constant (Figure 7A), both slopes and intercepts vary. An identical pattern is obtained when $1/v$ is plotted versus 1/MgATP at several fixed concentrations of $Mg^{2+}$, keeping poly($E_4Y$) concentration constant (Figure 7B). None of the replots of slope versus 1/MgATP or $1/Mg^{2+}$ go through the origin. These results are consistent with a random order of addition of MgATP with respect to $Mg^{2+}$ but do not rule out an ordered addition in which $K_{ia}K_b = K_aK_{ib}$. When poly($E_4Y$) and $Mg^{2+}$ are considered (Figure 6), the results indicate that binding of the two substrates, $Mg^{2+}$ and poly($E_4Y$), is ordered with $Mg^{2+}$ adding prior to poly($E_4Y$).

These results taken together indicate that the free enzyme can bind either MgATP first followed by binding to free $Mg^{2+}$ or vice versa (Scheme 1). On the other hand, poly($E_4Y$) can only add to the enzyme after MgATP and $Mg^{2+}$.

*Inhibition by AMP−PCP.* To verify the order of substrate binding, AMP−PCP was used as a dead-end ATP analogue. Coupled spectrophotometric assay was used in these experiments. AMP−PCP was a competitive inhibitor versus ATP as well as poly($E_4Y$) (Figure 8). These results are fully consistent and confirm an ordered substrate addition in which MgATP binds before poly($E_4Y$) (Scheme 1). A random kinetic mechanism predicts that the pattern of enzyme inhibition by AMP−PCP would be competitive versus ATP and noncompetitive versus the peptide substrate. Thus these results are inconsistent with a random kinetic mechanism.

*Product Inhibition.* Product inhibition studies were undertaken to address the order of product release. Because of incompatibility of MgADP with the coupled spectrophotometric assay, the radioactive assay was used in these experiments. MgADP was found to be a competitive inhibitor with respect to MgATP, indicating that both MgATP and MgADP bind to the same form of the enzyme, the free enzyme (Figure 9A). On the other hand, MgADP was a noncompetitive inhibitor with respect to poly($E_4Y$), indicating that MgADP and poly($E_4Y$) bind to different forms of the enzyme (Figure 9B). These results are consistent with an ordered mechanism or a fully random kinetic mechanism for product release. However, these results taken together with substrate kinetics data as well as AMP−PCP inhibition data indicate that product release is ordered with MgADP being the last product released (Scheme 1).

## DISCUSSION

Angiogenesis has recently been recognized as the potential target for treatment of many diseases, especially cancer (*1*). Although angiogenesis seems to be a very complex process, recent evidence pinpoints VEGFR2 TK (a type II receptor) as one of the key molecules involved in initiating this process, presumably through activation of a phosphorylation cascade upon binding to VEGF (*16*).

The outline of the signal transduction pathways governing growth factor/receptor systems has emerged from recent genetic, biochemical, and structural data (*17*). According to this model, binding of a hormone or a growth factor (VEGF in this case) to its receptor (VEGFR2 TK) on the surface of the cells converts the receptor from a dormant state into an active state. This conversion involves phosphorylation of the receptor: ligand binding promotes receptor dimerization which leads to autophosphorylation resulting in formation of an active phosphorylated receptor.

There are several mechanisms by which receptor phosphorylation initiates a signal transduction pathway (*8*, *17*). First, the enzymatic activity of the cytosolic domain of the receptor is increased upon phosphorylation. An increase in the kinase activity of the receptor can directly lead to the initiation of a signal transduction pathway. Second, phosphorylation of some residues in the receptor creates binding sites for proteins containing the *src* homology-2 (SH2) domain, thereby recruiting these proteins. These SH2-

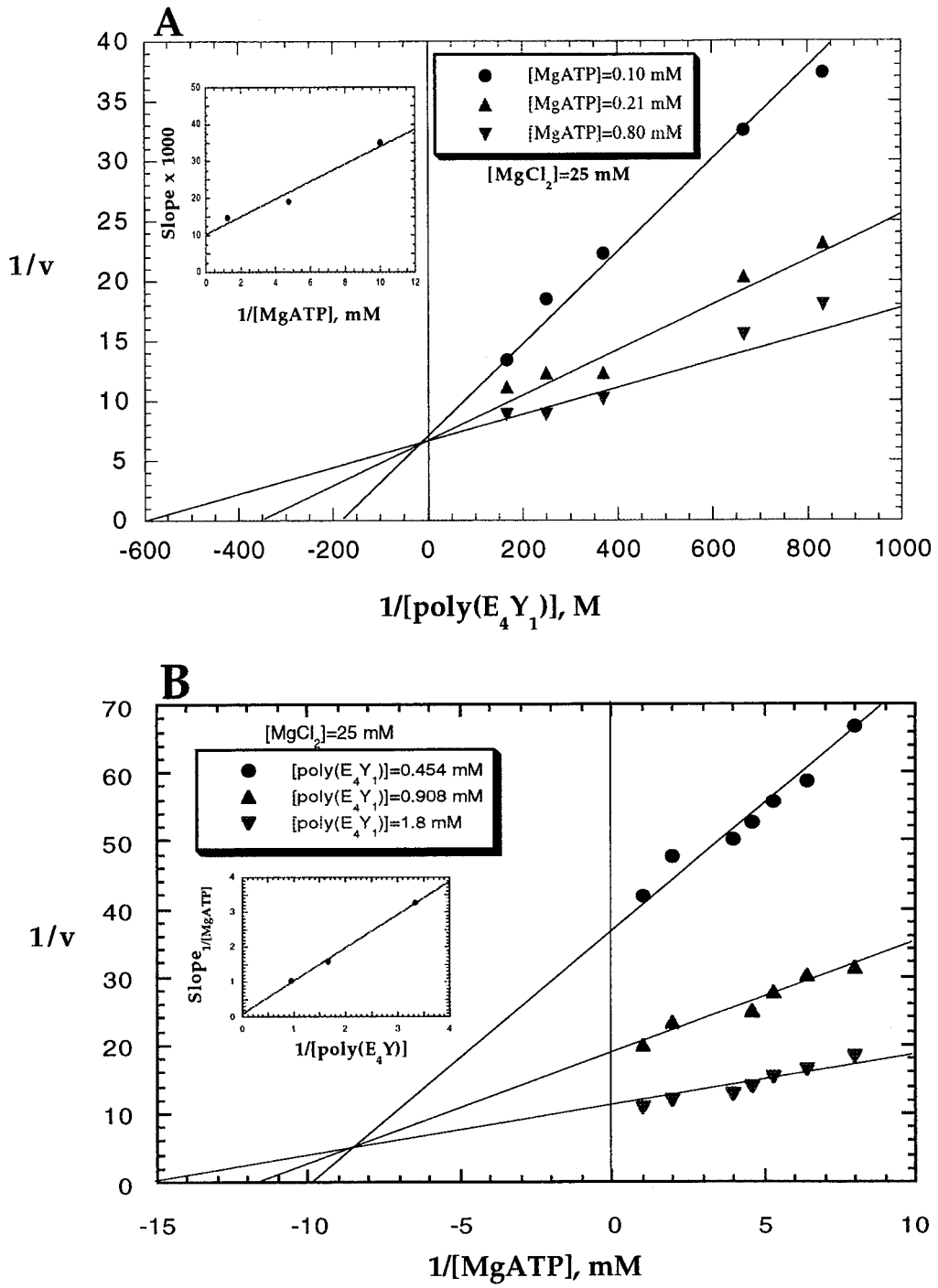


FIGURE 5: (A) Plot of $1/v$ vs 1/ [poly($E_4Y_1$)] at three fixed concentrations of MgATP and one fixed concentration of $Mg^{2+}$, 25 mM. Inset: Plot of slope from A vs 1/[MgATP]. (B) Plot of $1/v$ vs 1/[MgATP] at three fixed concentrations of poly($E_4Y_1$) and one fixed concentration of $Mg^{2+}$, 25 mM. Inset: Plot of slope from B vs 1/[poly($E_4Y_1$)]. The unit for velocity ($v$) is expressed in $\Delta OD_{@340\ nm}$/min.

containing proteins may have enzymatic activity themselves, often kinase or phosphatase, which could initiate a phosphorylation cascade. Alternatively, the SH2-containing proteins may have other domains which would recruit yet other proteins involved in the generation of a phosphorylation cascade. Hence, binding of SH2-domain-containing proteins to receptors would be expected to increase the effective local concentration of these physiological substrates or their associated partners and thereby accelerate their phosphorylation rate under physiological conditions.

Our results indicate that cchVEGFR2 TK catalyzes its autophosphorylation by a trans mechanism. Since cch-VEGFR2 TK lacks the ligand-binding domain, it catalyzes its autophosphorylation in a ligand-independent manner. This observation is predicted by the ligand-induced autophosphorylation model. According to this model, the sole function of the ligand is to promote dimerization. Therefore, in the absence of the ligand-binding domain, autophosphorylation should become enzyme-concentration-dependent because the autophosphorylation reaction still occurs via the same mechanism: trans. Using a similar experimental approach, a trans mechanism of autophosphorylation has been shown for IRTK and FGFR TK (*7*, *18*, *19*). A combination of cis and trans mechanisms has been proposed for autophospho-

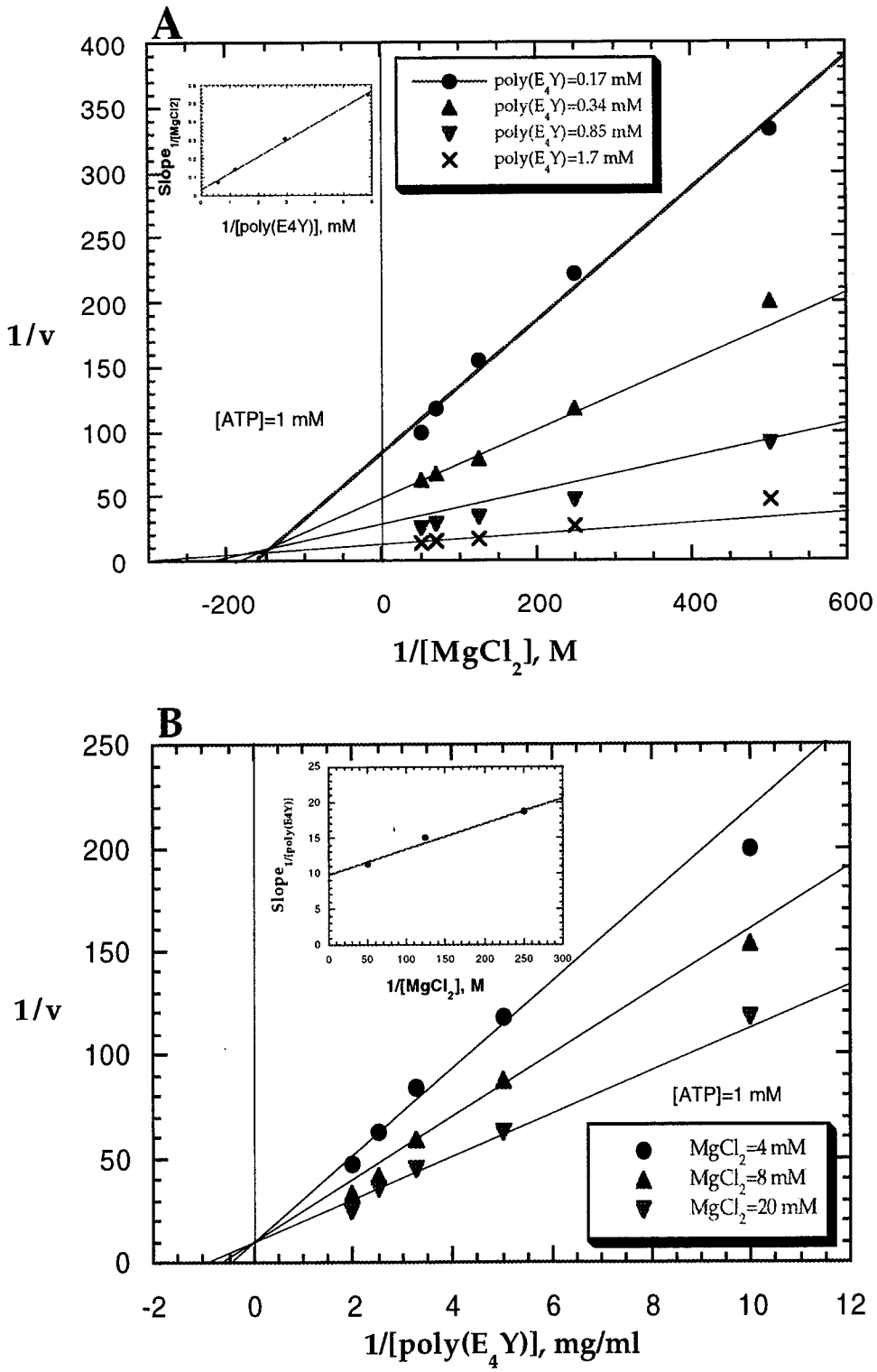


FIGURE 6: (A) Plot of $1/v$ vs $1/ Mg^{2+}$ at four fixed concentrations of poly($E_4Y_1$) and one fixed concentration of MgATP. Inset: Plot of slope from A vs 1/[poly($E_4Y_1$)]. (B) Plot of $1/v$ vs 1/[poly($E_4Y_1$)] at three fixed concentrations of $Mg^{2+}$ and one fixed concentration of MgATP. Inset: Plot of slope from B vs $1/[Mg^{2+}]$. The unit for velocity ($v$) is expressed in $\Delta OD_{@340\ nm}$/min.

rylation of TrkB tyrosine kinase (TrkB TK) (*20*).

Within the tyrosine kinase family of receptors, autophosphorylation is associated with an increase in the enzymatic activity of the receptors with respect to phosphorylation of the exogenous substrate. Phosphorylated cchVEGFR2 TK exhibits 2−3-fold higher $k_{cat}$ values relative to the unphosphorylated form. Enzyme phosphorylation also affects the affinity of the enzyme for all of its substrates by lowering their $K_M$. Overall, enzyme phosphorylation improves the catalytic efficiency ($k_{cat}/K_M$) of the enzyme by a factor of 10. Similar results have been reported for IRTK (*6*).

Autophosphorylation presumably brings about a conformational change in the enzyme which leads to optimal disposition of residues in and around the active site. These changes are reflected in the altered $k_{cat}$ and $K_M$ values of p-cchVEGFR2 TK relative to those of native cchVEGFR2 TK. In addition to increased catalytic efficiency, p-cchVEGFR2 TK is also more stable and exhibits better solution

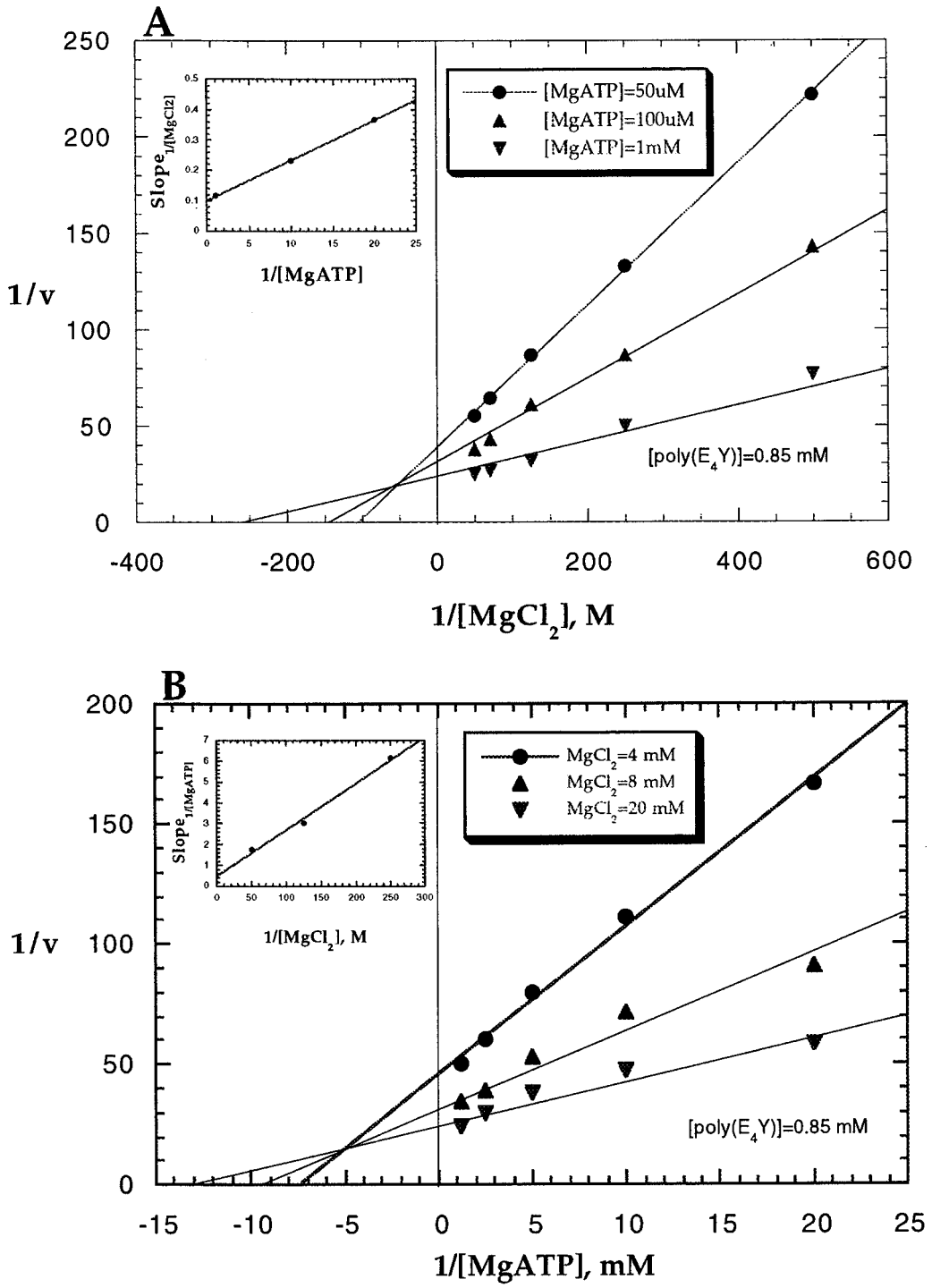


FIGURE 7: (A) Plot of 1/v vs 1/[$Mg^{2+}$], at three fixed concentrations of MgATP and one fixed concentration of poly($E_4Y_1$). Inset: Plot of slope from A vs 1/[MgATP]. (B) Plot of 1/$v$ vs 1/[MgATP] at three fixed concentrations of $Mg^{2+}$ and one fixed concentration of poly-($E_4Y_1$). Inset: Plot of slope from B vs 1/[$Mg^{2+}$]. The unit for velocity ($v$) is expressed in $\Delta OD_{@340\ nm}$/min.

properties, as judged by native gel and light-scattering experiments, compared with the nonphosphorylated form (data not shown).

Autophosphorylation introduces 5 or 6 phosphate groups per molecule of cchVEGFR2 TK. The existence of multiple phosphorylation sites per receptor (within the catalytic domain) is well-precedented. Five and seven phosphorylation sites have been identified in IRTK and FGFR TK, respectively (*21*, *22*). The reason for the existence of multiple phosphorylation sites is not clear. In IRTK, phosphorylation of three residues within the activation loop correlates with an increase in kinase activity (*23*). The correlation of phosphorylation of the activation loop and the increase in the enzymatic activity have been proposed to be a general feature of the tyrosine kinase receptor family (*24*). In FGFR TK, phosphorylation of one tyrosine residue creates a major site for interaction with the SH2 domain of phospholipase C-$\gamma$l (PLC-$\gamma$l) (*19*). As in FGFR TK, another general feature of the tyrosine kinase receptor family appears to be the generation of an SH2-binding site by phosphorylation of some tyrosine residues within the receptor molecules (*17*). Thus the existence of multiple phosphorylation site

Scheme 1: The Kinetic Mechanism for cchVEGFR2 TK: A Rapid Equilibrium Hybrid Random-Ordered Terreactant System

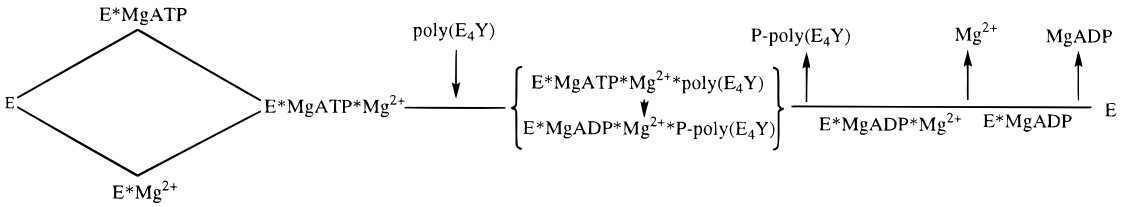


in cchVEGFR2 TK can readily be explained in terms of the general features proposed for these receptors. Additionally, phosphorylation of some residues may impart yet uncharacterized properties to cchVEGFR2 TK.

A detailed understanding of the kinetic as well as the chemical mechanisms by which this enzyme catalyzes its reaction is necessary for the rational design of potent inhibitors against this receptor. Hence, we have attempted to establish the kinetic mechanism of this enzyme as the first step toward understanding its chemical mechanism.

The order of substrate addition must be addressed to establish the kinetic mechanism of a multisubstrate enzyme. Steady-state kinetics is the commonly employed method for determining the kinetic mechanism of an enzyme (*10*, *25*). The kinetic data obtained for cchVEGFR2 TK clearly rule out a ping-pong mechanism for this reaction since none of the velocity line patterns were parallel, indicating that there is no kinetically irreversible step between the binding of any of the substrates. These results indicate that the enzyme binds its substrates in a semi-ordered fashion: the free enzyme can bind either MgATP first followed by binding to free $Mg^{2+}$ or vice versa (Scheme 1). On the other hand, poly($E_4$Y) can only add after MgATP and $Mg^{2+}$. Furthermore, product inhibition studies indicated that product release is ordered with MgADP being released last.

The kinetic mechanisms of several tyrosine kinases have been investigated. The kinetic mechanisms of *src* tyrosine kinase ($pp60^{c-src}$) (*26*), Csk tyrosine kinase (*27*, *28*), and insulin receptor tyrosine kinase (*29*) have been found to be random. The kinetic mechanism of v-*src* tyrosine kinase has been concluded to be ordered with MgATP binding first (*30*). There have been two reports on the kinetic mechanism of epidermal growth factor receptor tyrosine kinase (EGFR TK) (*31*, *32*). One study found the order of addition of substrate in EGFR TK to be random while the second study found it to be ordered with the peptide substrate binding first.

Among the protein kinases, cAMP-dependent protein kinase (cAPK), a serine/threonine kinase, is the most well-studied enzyme. Two different kinetic mechanisms have been proposed for cAPK. According to one mechanism, the enzyme catalyzes its reaction via a random addition of substrates and an ordered release of products (*33*). According to a second mechanism, the reaction proceeds via ordered sequential mechanism with MgATP binding first (*34*, *35*). These results have been reconciled in terms of a preferred order of binding with MgATP adding first. The kinetic mechanism for p38 mitogen activated protein kinase (MAP kinase) has been shown to be ordered with the protein substrate adding first (*36*).

These studies indicate that there is no conservation of the kinetic mechanism between tyrosine kinases and serine/threonine kinases or among each family of tyrosine kinases or serine/threonine kinases. Therefore, there are significant differences between these related enzymes, and their kinetic mechanisms should be determined individually. It should be noted that most of the kinetic mechanisms have been determined using peptide substrates. It is possible that these enzymes may function via a different kinetic mechanism with respect to their physiological protein substrates.

An important question for all kinases is their divalent metal requirement ($Mg^{2+}$/$Mn^{2+}$). It is generally accepted that the metal functions to form MgATP/MnATP, the true substrate, for these enzymes. In the case of tyrosine kinases, the concentrations of $Mg^{2+}$ required for the enzyme activity (~10 mM) far exceed the concentrations necessary for the formation of MgATP. In the case of cchVEGFR2 TK, 20 and 50 mM $Mg^{2+}$ was required for optimal enzyme activity for the phosphorylated and nonphosphorylated forms of the enzyme, respectively. A high metal concentration requirement has generally been taken as evidence for existence of a second role for the metal (*13*, *14*). Therefore, our results with cchVEGFR2 TK suggest a dual role for the divalent metal: chelation to ATP to form MgATP/MnATP and binding to another site whose function is generally to assist in catalysis. We have sought to provide kinetic evidence for the existence of the second metal-binding site on cchVEGFR2 TK. $Cd^{2+}$ was found to be a potent inhibitor of cchVEGFR2 TK. Enzyme inhibition studies indicate that $Cd^{2+}$ binds to a second metal-binding site on the enzyme.

Among the protein kinases, cAMP-dependent protein kinase (cAPK), a serine/threonine kinase, is the most well-studied enzyme, and subsequently, it has served as the paradigm for protein kinases in terms of both structure and catalytic function. An important difference between cAPK and cchVEGFR2 TK is their different metal requirement. Both NMR and crystal structure determination have shown that there are two metal-binding sites in cAPK: both metals are located in the active site and are chelated to ATP (*37*−*39*). The first metal binding activates the enzyme while the second metal binding is inhibitory. In the case of cchVEGFR2 TK, kinetic studies presented here are indicative of the existence of two metal-binding sites: one for chelation to ATP and a second metal whose binding is essential for catalysis. This is in contrast to cAPK where the second metal binding is inhibitory.

There is no structural data available for cchVEGFR2 TK. Therefore, the location of the second metal-binding site is not known. However, it is tempting to hypothesize that the second metal is involved in catalysis directly via interaction with ATP in the active site. If this hypothesis is correct, then one would expect a different coordination state for this metal in cchVEGFR2 TK compared to the coordination of the second metal in cAPK.

The ternary structure of the catalytic domain of activated insulin receptor tyrosine kinase (IRTK), complexed with peptide substrate and an ATP analogue (AMP−PNP), has

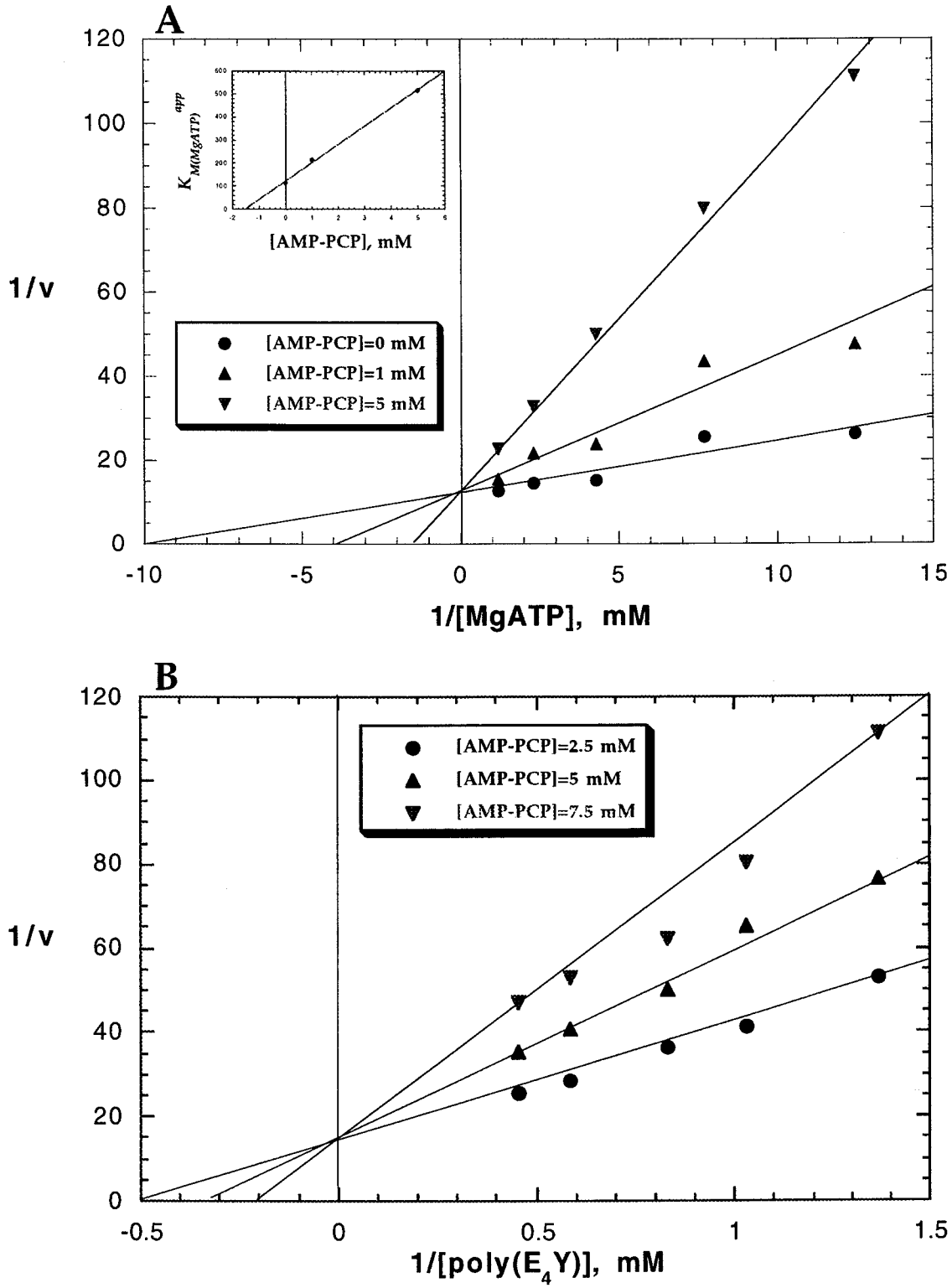


FIGURE 8: Kinetics of enzyme inhibition by AMP−PCP. (A) Plot of $1/v$ vs 1/[MgATP] at three fixed concentrations of AMP−PCP and one fixed concentration of poly($E_4Y_1$), 0.9 mM. (B) Plot of $1/v$ vs 1/ [poly($E_4Y_1$)] at three fixed concentrations of AMP−PCP and one fixed concentration of MgATP, 1 mM. The unit for velocity ($v$) is expressed in $\Delta OD_{@340\ nm}$/min. The calculated value of $K_I$ for AMP−PCP was varied from 360 $\mu$M to 1.3 mM, depending on the freshness of the AMP−PCP solutions. Freshly prepared solutions gave values in the range of 400 $\mu$M while solutions stored for more than a month at −20 °C gave higher values, presumably due to breakdown of AMP−PCP.

recently been reported (*40*). According to this structure, there are in fact two metals in the active site of IRTK. However, the coordination state of the second metal is different in IRTK than that in cAPK. As in cAPK, the first metal is coordinated to $\beta$- and $\gamma$-phosphates of ATP in IRTK. However, unlike cAPK, the second metal is coordinated only to the $\beta$-phosphate of ATP in IRTK. In cAPK, the second metal is coordinated to $\alpha$- and $\gamma$-phosphates of ATP.

In cAPK, the second metal was found to bridge the enzyme to the metal-nucleotide substrate (*37*). This observation may explain the inhibitory property of the second metal binding. In fact, pre-steady-state kinetic analysis indicated that the

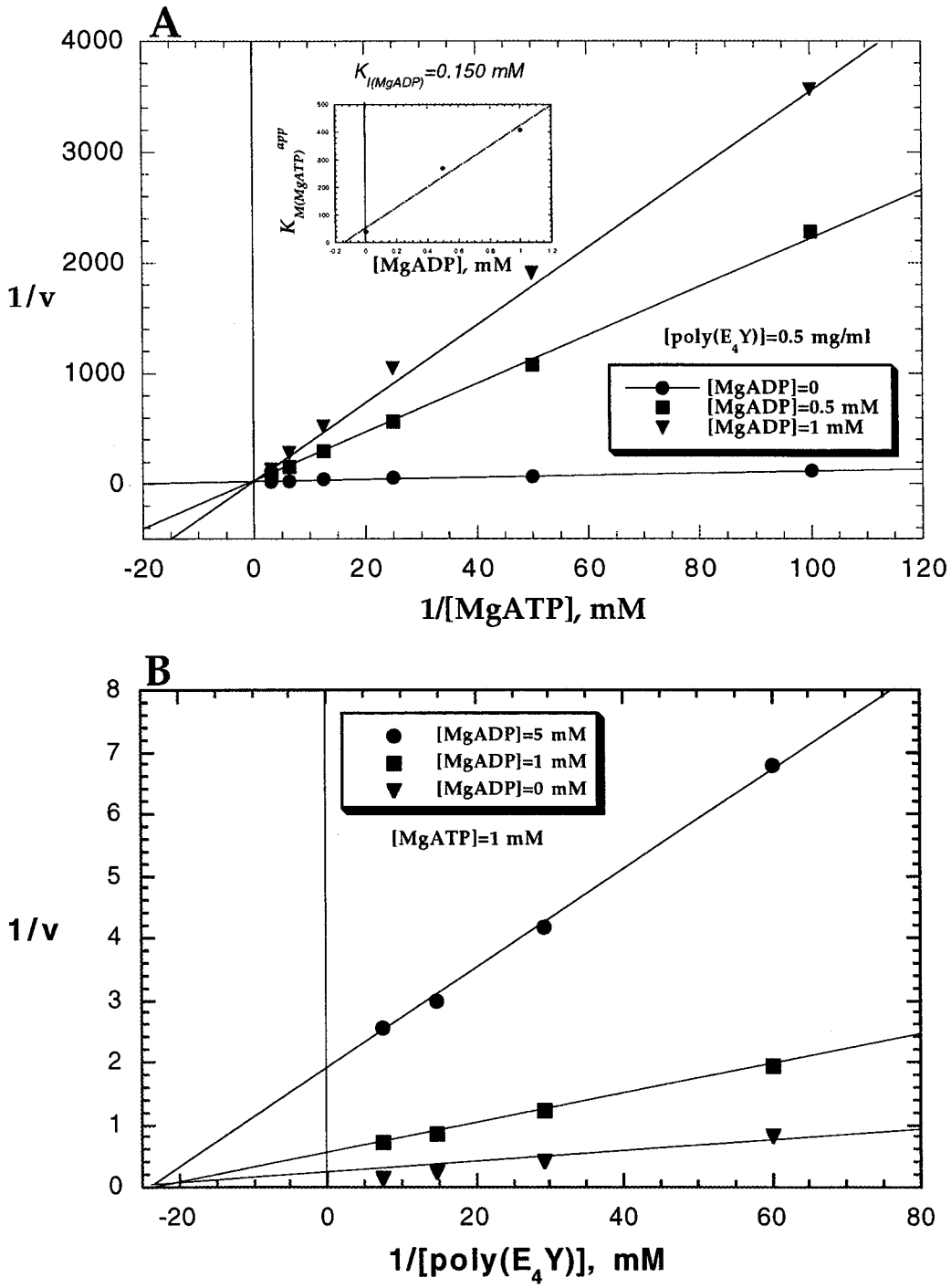


FIGURE 9: Product inhibition by MgADP. (A) Plot of $1/v$ vs 1/[MgATP] at three fixed MgADP concentrations and one fixed concentration of poly($E_4Y_1$), 0.8 mM, and $Mg^{2+}$, 25 mM. (B) Plot of $1/v$ vs 1/[poly($E_4Y_1$)] at three fixed MgADP concentrations and one fixed concentration of MgATP, 1 mM, and $Mg^{2+}$, 25 mM. The unit for velocity ($v$) is expressed in cpm (the amount of radioactivity incorporated into the substrate).

product release (ADP) was the rate-limiting step in the overall reaction (*41*), consistent with bridging of the nucleotide to the enzyme by the second metal. Ligation of the second metal in IRTK is different from that in cAPK. It is reasonable to assume that the binding of the second metal in IRTK would have a stimulatory effect on catalysis. In fact, kinetic studies have been reported for IRTK with respect to the role of the second metal binding on catalysis (*29*). These studies indicate that the second metal functions as an activator for the enzyme.

Since there is a great deal of homology within the tyrosine kinase family, it is reasonable to assume that cchVEGFR2 TK functions via mechanism similar to that of IRTK. The crystal structure of IRTK is fully consistent with the results presented here for cchVEGFR2 TK and further corroborates the existence of a second metal binding site which functions as an activator of the enzyme. The function of the second metal as the activator is a unique feature of cchVEGFR2 TK and IRTK which distinguishes them from cAPK. This feature may be a general property of the tyrosine kinase

family of enzymes. In fact, it has been suggested that several other tyrosine kinases also require a second metal for their activity (*42*). This is an important distinguishing feature between the tyrosine kinase family and the serine/threonine kinase family and may be utilized in the design of inhibitors specific for these enzymes.

It is important to note that no physiological substrate for cchVEGFR2 TK has been identified conclusively. Our results presented here have been obtained by using a synthetic peptide substrate, poly($E_4Y$). Although poly($E_4Y$) is efficiently phosphorylated by this enzyme, physiological relevance as well as its suitability as a substrate must be addressed. Since poly($E_4Y$) lacks recognition elements such as *src* homology-2 (SH2), *src* homology-3 (SH3), and pleckstrin homology (PH) domain, its phosphorylation will not be subject to regulation involving these elements. Therefore, studies presented here using poly($E_4Y$) as substrate will not be useful in deciphering those interactions. On the other hand, the lack of SH2, SH3, and PH domains (*17*) in poly($E_4Y$) may simplify the interpretation of our results and shed some light on the regulation of the activity of this receptor by autophosphorylation in the absence of these recognition elements. Using poly($E_4Y$) as substrate, autophosphorylation increases the catalytic efficiency of the enzyme by a factor of 10 by affecting $k_{cat}$ and $K_M$ for both substrates. If these conclusions are valid for physiological substrates, subtle changes in the catalytic properties of this enzyme upon phosphorylation may play a significant role in the regulation of the activity of this receptor.

## ACKNOWLEDGMENT

The authors would like to thank Rich Showalter and Mike Gehring for the cloning of cchVEGFR2 TK.

## REFERENCES

1. Folkman, J., and Shing, Y. (1992) *J. Biol. Chem. 267*, 10931−10934.
2. Eckhadt, S. G., and Pluda, J. M. (1997) *Invest. New Drugs 15*, 1−3.
3. O'Reilly, M. S. (1997) *Invest. New Drugs 15*, 5−13.
4. Terman, B. I., Dougher-Vermazen, M., Carrion, M. E., Dimitrov, D., Armellino, D. C., Gospodarowicz, D., and Bohlen, P. (1992) *Biochem. Biophys. Res. Commun. 187*, 1579−1586.
5. Nguyen, M. (1997) *Invest. New Drugs 15*, 29−37.
6. Wei, L., Hubbard, S. R., Hendrickson, W. A., and Ellis, L. (1995) *J. Biol. Chem. 270*, 8122−8130.
7. Cobb, M. H., Sang, B.-C., Gonzalez, R., Goldsmith, E., and Ellis, L. (1989) *J. Biol. Chem. 264*, 18701−18706.
8. Ullrich, A., and Schlessinger, J. (1990) *Cell 61*, 203-212.
9. Mohammadi, M., Schlessinger, J., and Hubbard, S. R. (1996) *Cell 86*, 577−587.
10. Cleland, W. W. (1979) *Methods Enzymol. 63*, 103.
11. Doughter-Vermazen, M., Hulmes, J. D., Bohlen, P., and Terman, B. I. (1994) *Biochem. Biophys. Res. Commun. 205*, 728−738.
12. Villafranca, J. J., and Nowak, T. (1992) *The Enzymes XX*, 63−94.
13. McClure, W. R., Lardy, H. A., and Kneifel, H. P. (1971) *J. Biol. Chem. 246*, 3569−3578.
14. Infante, J. P., and Kinsella, J. E. (1976) *Int. J. Biochem. 7*, 483−496.
15. Dawson, R. M. C., Elliott, D. C., Elliott, W. H., and Jones, K. M. (1986) *Data for Biochemical Research, 3rd ed., Oxford Science Publications*, pp 399−415.
16. Thomas, K. A. (1996) *J. Biol. Chem. 271*, 603−606.
17. Pawson, T. (1995) *Nature 373*, 573−580.
18. Frattali, A. L., Treadway, J. L., and Pessin, J. E. (1992) *J. Biol. Chem. 267*, 19521−19528.
19. Jaye, M., Schlessinger, J., and Dionne, C. (1992) *Biochim. Biophys. Acta 1135*, 185−199.
20. Iwasaki, Y., Nishiyama, H., Suzuki, K., and Koizumi, S. (1997) *Biochemistry 36*, 2694−2700.
21. Kohanski, R. A. (1993) *Biochemistry 32*, 5773−5780.
22. Mohammadi, M., Dikic, I., Sorokin, A., Burgess, W. H., Jaye, M., and Schlessinger, J. (1996) *Mol. Cell. Biol. 16*, 977−989.
23. Wilden, P. A., Kahn, C. R., Siddle, K., and White, M. F. (1992) *J. Biol. Chem. 267*, 16660−16668.
24. Johnson, L. N., Noble, M. E. M., and Owen, D. J. (1996) *Cell 85*, 149−158.
25. Cleland, W. W. (1982) *Methods Enzymol. 87*, 159−179.
26. Boerner, R. J., Barker, S. C., and Knight, W. B. (1995) *Biochemistry 34*, 16419−16423.
27. Cole, P. A., Burns, P., Takacs, B., and Walsh, C. T. (1994) *J. Biol. Chem. 269*, 30880−30887.
28. Grace, M. R., Walsh, C. T., and Cole, P. A. (1997) *Biochemistry 36*, 1874−1881.
29. Walker, D. H., Kuppuswamy, D., Visvanathan, A., and Pike, L. (1987) *Biochemistry 26*, 1428−1433.
30. Wong, T. W., and Goldberg, A. R. (1984) *J. Biol. Chem. 259*, 3127−3131.
31. Posner, I., Engel, M., and Levitski, A. (1992) *J. Biol. Chem. 267*, 20638−20647.
32. Erneux, C., Cohen, S., and Garbers, D. L. (1983) *J. Biol. Chem. 258*, 4137−4142.
33. Cook, P. F., Neville, M. E., Jr., Vrana, K. E., Hartle, T., and Roskoski, R., Jr. (1982) *Biochemistry 21*, 5794−5799.
34. Whitehouse, S., and Walsh, D. A. (1983) *J. Biol. Chem. 258*, 3682−3692.
35. Whitehouse, S., Feramisco, J. R., Casnellie, J. E., Krebs, E. G., and Walsh, D. A. (1983) *J. Biol. Chem. 258*, 3693−3701.
36. LaGrasso, P. V., Frantz, B., Ronaldo, A. M., O'Keefe, S. J., Hermes, J. D., and O'Neil, E. A. (1987) *Biochemistry 36*, 10422−10427.
37. Armstrong, R. N., Kondo, H., Granot, J., Kaiser, E. T., and Mildvan, A. S. (1979) *Biochemistry 18*, 1230−1238.
38. Bossemeyer, D., Engh, R. A., Kinzel, V., Ponstingl, H., and Hubber, R. (1993) *EMBO J. 12*, 849−859.
39. Zheng, J., Trafny, E. A., Knighton, D. R., Xuong, N. H., Taylor, S. S., Ten Eyck, L. F., and Sowadski, J. M. (1993) *Acta Crystallogr., Sect. D 49*, 362−365.
40. Hubbard, S. R., Wei, L., Ellis, L., and Hendrickson, W. A. (1994) *Nature 372*, 746−754.
41. Grant, B. D., and Adams, J. A. (1996) *Biochemistry 35*, 2022−2029.
42. Sun, G., and Budde, R. J. A. (1997) *Biochemistry 36*, 2139−2146.

BI981291F